Supporting Information:

Synthesis of mesoporous TiO_2@C@MnO_2 multi-shelled hollow nanospheres with high rate capability and stability for lithium-ion batteries

Li Liu,‡[a] Jun Peng,‡[a] Gang Wang[a*], Yanqing Ma[a], Feng Yu[a*], Bin Dai[a], Xu-Hong Guo[a,b] and Ching-Ping Wong[c,d]

[a] *School of Chemistry and Chemical Engineering, Key Laboratory of Materials-Oriented Chemical Engineering of Xinjiang Uygur Autonomous Region, Shihezi University, Shihezi, P.R. China. Email:gwangshzu@163.com, yufeng05@mail.ipc.ac.cn*

[b] *State Key Laboratory of Chemical Engineering, East China University of Science and Technology, Shanghai 200237, P. R. China*

[c] *Department of Electronic Engineering, The Chinese University of Hong Kong, Shatin, NewTerritories, HongKong, SAR, China*

[d] *School of Materials Science and Engineering, Georgia Institute of Technology, Atlanta, GA, 30332, United States*

‡These authors contributed equally to this work.

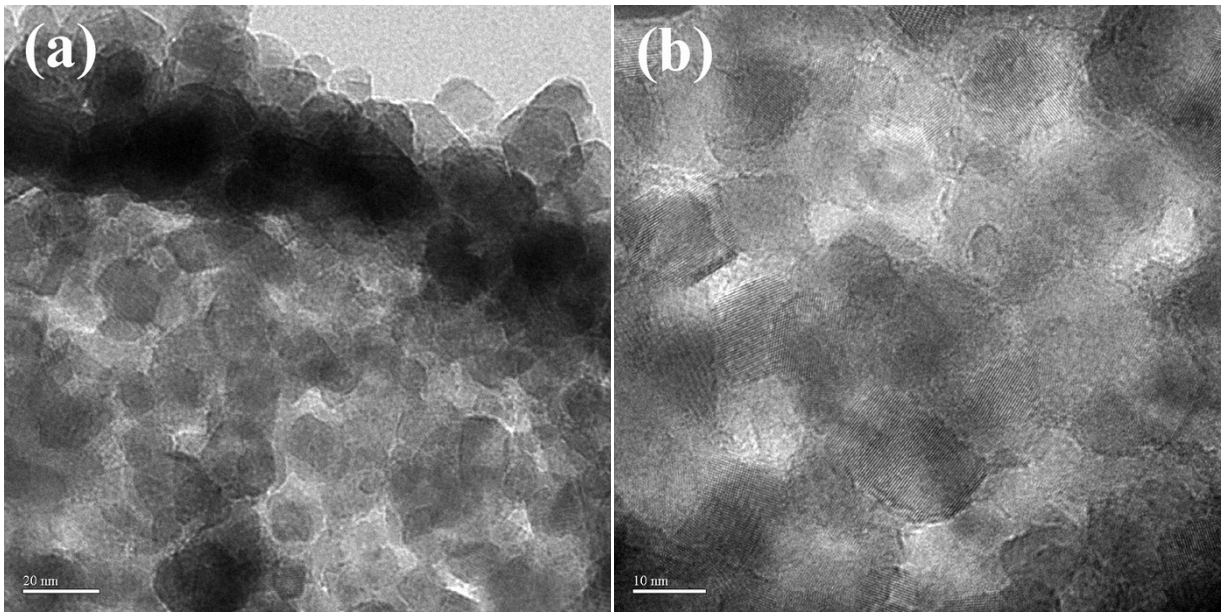

Figure S1 (a) Magnified TEM image of a single TiO_2 HNSs; (b) HRTEM image of the shell of TiO_2 HNSs

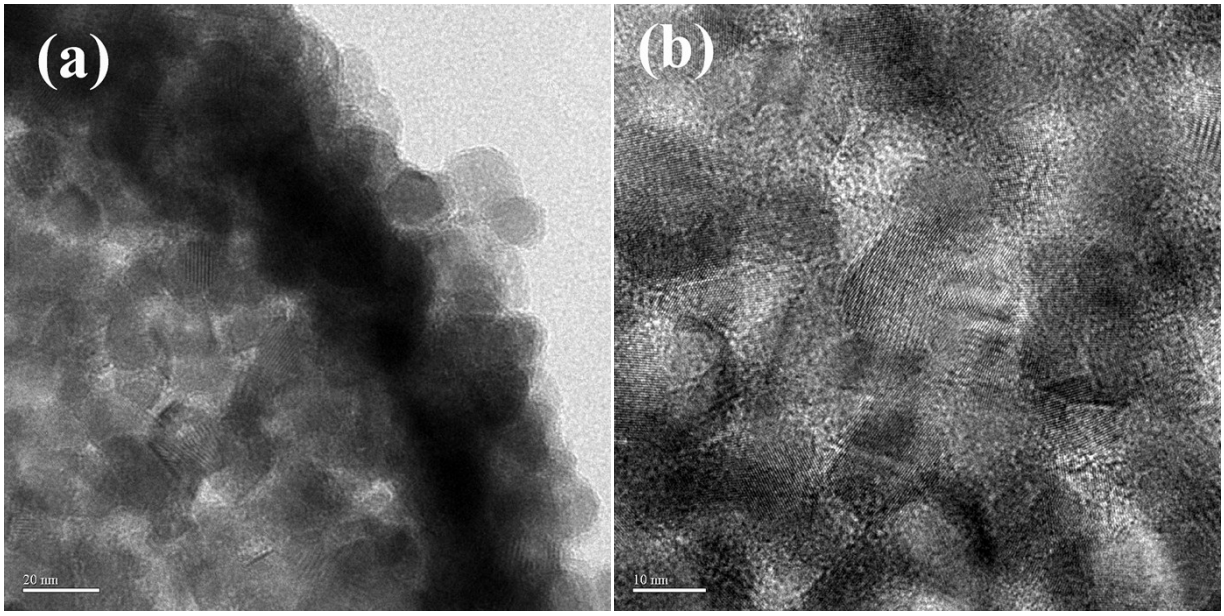

Figure S2 (a) Magnified TEM image of a single TiO_2@C HNSs; (b) HRTEM image of the shell of TiO_2@C HNSs

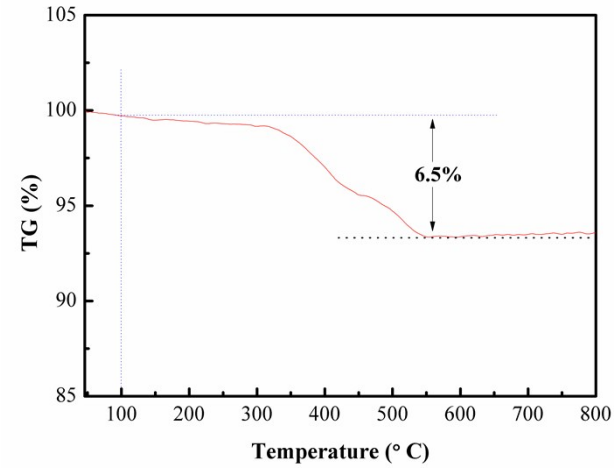

Figure S3 Thermogravimetric analysis of TiO_2@C HNSs.

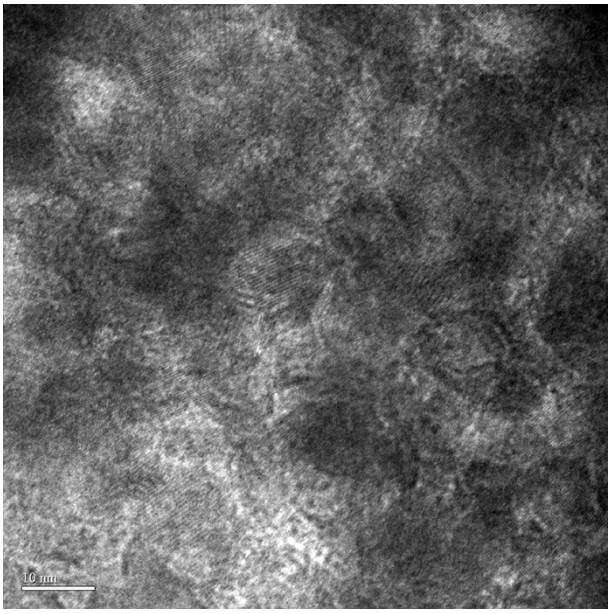

Figure S4 HRTEM image of the shell of TiO_2@C@MnO_2 HNSs

Table S1. The relative MnO_2 composition of TiO_2@C@MnO_2 HNSs samples.

Samples	The concentrations of $KMnO_4$ [mol L^{-1}]	MnO_2 contents in the TiO_2@C@MnO_2 [wt.%]	The ration of TiO_2/MnO_2
a	0.008	9.1	9.43
b	0.016	17.8	4.82
c	0.04	29.7	2.89

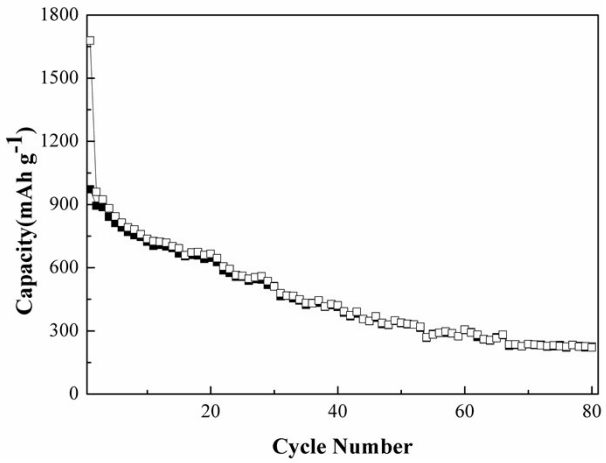

Figure.S5 Cycling performance of the bare MnO_2 HNSs at a current density of 100mA g^{-1}

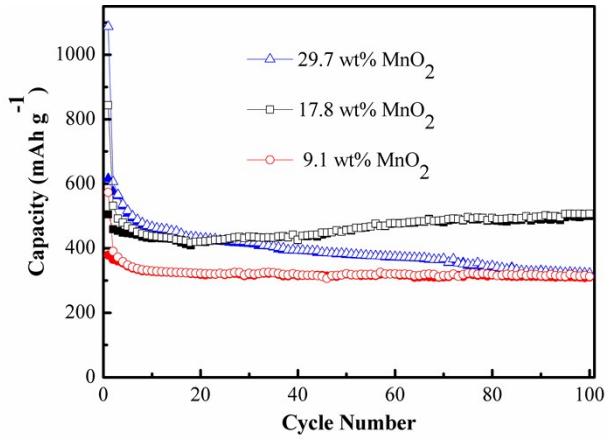

Figure S6 Cycling performance of TiO_2@C@MnO_2 with different account of MnO_2 at a current density of 100 mA g^{-1}

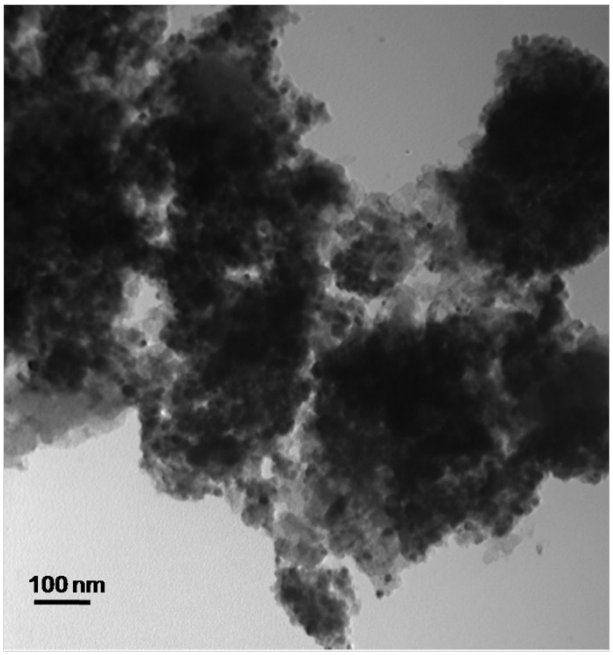

Figure S7 TEM image of the TiO_2@C@MnO_2 (29.7 wt% MnO_2) after 100th cycles.

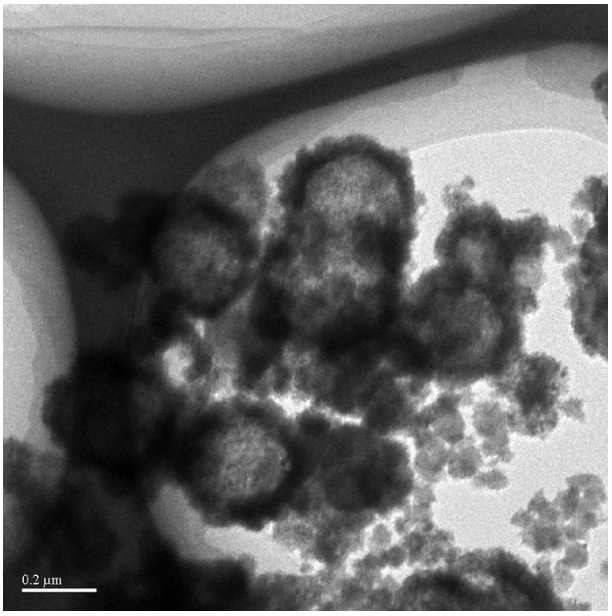

Figure S8 TEM image of the TiO_2@C@MnO_2 (17.8 wt% MnO_2) after the rate cycling test.

Table S2 List of recent work on TiO_2 based composites as the lithium-ion battery electrode.

Typical examples	Cycling Performance	Rate Performance	Ref
TiO_2@C@MnO_2 multi-shelled HNSs	506.8 mAh g^{-1} at 100 mA g^{-1} (100 cycles) 284.6 mAh g^{-1} at 1.0 A g^{-1} (200 cycles)	242.5 mAh g^{-1} at 3.35 A g^{-1} 196.6 mAh g^{-1} at 6.7 A g^{-1} 149.9 mAh g^{-1} at 10 A g^{-1}	This work
TNAs@MnO_2 nanosheets	610 mAh g^{-1} at 0.35 A g^{-1} (100 cycles) 320 mAh g^{-1} at 0.7 A g^{-1} (100 cycles) 385 mAh g^{-1} at 0.7 A g^{-1} (700 cycles)	695 mAh g^{-1} at 0.14 A g^{-1} 400 mAh g^{-1} at 0.7 A g^{-1} 55 mAh g^{-1} at 3.5 A g^{-1}	[53]
TiO_2-MnO_2/MnO_2 heterostructures	888 mAh g^{-1} at 0.1 A g^{-1} (50 cycles) 185 mAh g^{-1} at 2 A g^{-1} (400 cycles)	347 mAh g^{-1} at 1 A g^{-1} 212 mAh g^{-1} at 2 A g^{-1} 122 mAh g^{-1} at 4 A g^{-1}	[17]
TiO_2-C/MnO_2 core-double-shell nanowire arrays	352 mAh g^{-1} at 0.335 A g^{-1} (100 cycles) 218 mAh g^{-1} at 3.35 A g^{-1} (150 cycles)	332 mAh g^{-1} at 0.67 A g^{-1} 235 mAh g^{-1} at 3.35 A g^{-1} 130 mAh g^{-1} at 10 A g^{-1}	[12]
TiO_2/SnO_2/C hollow microspheres	589.3 mAh g^{-1} at 0.2 A g^{-1} (550 cycles) 403.6 mAh g^{-1} at 0.8 A g^{-1} (500 cycles) 323.9 mAh g^{-1} at 2 A g^{-1} (500 cycles)	438.7 mAh g^{-1} at 0.4 A g^{-1} 371.3 mAh g^{-1} at 1 A g^{-1} 298.3 mAh g^{-1} at 3 A g^{-1}	[16]
TiO_2 nanotube @SnO_2 nanoflake	450 mAh g^{-1} at 1.6 A g^{-1} (50 cycles)	1400 mAh g^{-1} at 0.4 A g^{-1} 1000 mAh g^{-1} at 0.8 A g^{-1} 400 mAh g^{-1} at 3.2 A g^{-1}	[56]
TiO_2/SnO_2/Carbon hybrid nanofibers	438.9 mAh g^{-1} at 0.03 A g^{-1} (100 cycles)	313.9 mAh g^{-1} at 0.5A g^{-1} 198.36 mAh g^{-1} at 1 A g^{-1} 165 mAh g^{-1} at 2 A g^{-1}	[10]
TS@G	617 mAh g^{-1} at 0.4 A g^{-1} (700 cycles)	600 mAh g^{-1} at 0.5A g^{-1} 481 mAh g^{-1} at 1 A g^{-1}	[19]

		388 mAh g^{-1} at 1.5 A g^{-1}	
TiO_2–SnO_2/C double-shell nanotubes	354.3 mAh g^{-1} at 0.5 A g^{-1} (120 cycles) 256 mAh g^{-1} at 1 A g^{-1} (710 cycles)	350.3 mAh g^{-1} at 1A g^{-1} 100 mAh g^{-1} at 2 A g^{-1} 77 mAh g^{-1} at 5 A g^{-1}	[20]
TiO_2@Fe_2O_3 core–shell nanoframework arrays	430.2 mAh g^{-1} at 0.2 A g^{-1} (103 cycles)	401.6 mAh g^{-1} at 0.4A g^{-1} 268.4 mAh g^{-1} at 0.8 A g^{-1} 168.3 mAh g^{-1} at 1.6 A g^{-1}	[54]
TiO_2/Fe_2O_3 fiber-in-tube hierarchical heterostructures	642.5 mAh g^{-1} at 0.1 A g^{-1} (240 cycles)	261.8 mAh g^{-1} at 2A g^{-1} 143.3 mAh g^{-1} at 4 A g^{-1} 85.3 mAh g^{-1} at 6 A g^{-1}	[21]
TiO_2@Fe_2O_3 hollow nanostructures	530 mAh g^{-1} at 0.2 A g^{-1} (200 cycles)	490 mAh g^{-1} at 0.4A g^{-1} 440 mAh g^{-1} at 0.8 A g^{-1} 300 mAh g^{-1} at 1.6 A g^{-1}	[13]
TiO_2/Fe_3O_4-PG ternary heterostructures	703 mAh g^{-1} at 0.5 A g^{-1} (200 cycles) 524 mAh g^{-1} at 1 A g^{-1} (200 cycles)	264 mAh g^{-1} at 3A g^{-1} 219 mAh g^{-1} at 5 A g^{-1} 192 mAh g^{-1} at 8 A g^{-1}	[22]
TiO_2 nanowire@MoS_2 nanosheet	544 mAh g^{-1} at 0.1 A g^{-1} (100 cycles)	500 mAh g^{-1} at 0.4A g^{-1} 440 mAh g^{-1} at 0.8A g^{-1} 414 mAh g^{-1} at 1 A g^{-1}	[23]
TiO_2/$MnTiO_3$@C porous microspheres	402.6 mAh g^{-1} at 0.1 A g^{-1} (300 cycles)	200.4 mAh g^{-1} at 0.4A g^{-1} 150.5 mAh g^{-1} at 0.8A g^{-1} 103.3 mAh g^{-1} at 1.6 A g^{-1}	[19]
G-TiO_2@Co_3O_4 nanobelt arrays	437 mAh g^{-1} at 0.1 A g^{-1} (190 cycles)	345 mAh g^{-1} at 0.2A g^{-1} 250 mAh g^{-1} at 0.4A g^{-1} 204 mAh g^{-1} at 0.8 A g^{-1}	[11]
TiO_2@NiO core/shell nanosheet arrays	376.5 mAh g^{-1} at 0.2 A g^{-1} (100 cycles)	410mAh g^{-1} at 0.4A g^{-1} 250 mAh g^{-1} at 0.8A g^{-1} 199.2 mAh g^{-1} at 1.6 A g^{-1}	[49]
TiO_2@ZnO array	340.2 mAh g^{-1} at 0.2 A g^{-1} (100 cycles)	330mAh g^{-1} at 0.4A g^{-1} 253 mAh g^{-1} at 0.8A g^{-1} 205.2 mAh g^{-1} at1.6 A g^{-1}	[15]

Table S3 Kinetic Parameters of the TiO_2 HNSs, TiO_2@C HNSs and TiO_2@C@MnO_2 HNSs.

Materials	SEI film resistance (R_f)	Charge-transfer resistance (R_{ct})
TiO_2 HNSs	2.9 Ω	116.9 Ω
TiO_2@C HNSs	4.7 Ω	81.4 Ω
TiO_2@C@MnO_2 HNSs	3.7 Ω	51.8 Ω